AD-A261 726

HIGH FREQUENCY (HF) RADIOWAVE PROPAGATION

DTIC
S ELECTE
FEB 1 1993
C D

Gary S. Sales

University of Massachusetts Lowell
Center for Atmospheric Research
450 Aiken Street
Lowell, Massachusetts 01854
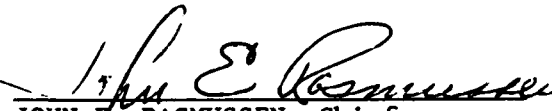
April 1992

Scientific Report #6

93

PHILLIPS LABORATORY
AIR FORCE SYSTEMS COMMAND
HANSCOM AIR FORCE BASE, MA 01731-5000
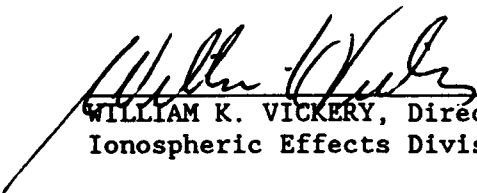
93-01762

This technical report has been reviewed and is approved for publication.

JÜRGEN BUCHAU
Contract Manager

JOHN E. RASMUSSEN, Chief
Ionospheric Application Branch

WILLIAM K. VICKERY, Director
Ionospheric Effects Division

This document has been reviewed by the ESD Public Affairs Office (PA) and is releasable to the National Technical Information Service (NTIS).

Qualified requestors may obtain additional copies from the Defense Technical Information Center. All others should apply to the National Technical Information Service.

If your address has changed, or if you wish to be removed from the mailing list, or if the addressee is no longer employed by your organization, please notify PL/TSI, Hanscom AFB, MA 01731-5000. This will assist us in maintaining a current mailing list.

Do not return copies of this report unless contractual obligations or notices on a specific document requires that it be returned.

REPORT DOCUMENTATION PAGE

Public reporting burden for this collection of information is estimated to average 1 hour per response, including the time for reviewing instructions, searching existing data sources, gathering and maintaining the data needed, and completing and reviewing the collection of information. Send comments regarding this burden estimate or any other aspect of this collection of information, including suggestions for reducing this burden, to Washington Headquarters Services, Directorate for Information Operations and Reports, 1215 Jefferson Davis Highway, Suite 1204, Arlington, VA 22202-4302, and to the Office of Management and Budget, Paperwork Reduction Project (0704-0188), Washington, DC 20503

1. AGENCY USE ONLY (Leave blank)	2. REPORT DATE April 1992	3. REPORT TYPE AND DATES COVERED Scientific Report #6

4. TITLE AND SUBTITLE

High Frequency (HF) Radiowave Propagation

5. FUNDING NUMBERS
PE 12417F
PR ESDO TA 01 WU AB
Contract
F19628-90-K-0029

6. AUTHOR(S)

Gary S. Sales

7. PERFORMING ORGANIZATION NAME(S) AND ADDRESS(ES)

University of Massachusetts Lowell
Center for Atmospheric Research
450 Aiken Street
Lowell, MA 01854

8. PERFORMING ORGANIZATION REPORT NUMBER

9. SPONSORING/MONITORING AGENCY NAME(S) AND ADDRESS(ES)

Phillips Laboratory
Hanscom AFB, MA 01731-5000

Contract Monitor: Jurgen Buchau/GPIS

10. SPONSORING/MONITORING AGENCY REPORT NUMBER

PL-TR-92-2123

11. SUPPLEMENTARY NOTES

12a. DISTRIBUTION/AVAILABILITY STATEMENT

Approved for public release;
distribution unlimited

12b. DISTRIBUTION CODE

13. ABSTRACT (Maximum 200 words)

This report serves to introduce the basics of high frequency radio-wave propagation in the earth's ionosphere. It is intended for people who are not fully acquainted with the physics of the problem but have had some experience working with or will have to work with over-the-horizon radar systems. This material, after an introduction to propagation theory and terminology, concentrates on the features of the OTH radar. First, backscatter ionogram is introduced as the primary diagnostic tool for the management of the radar in terms of the ionospheric environment. The synthesis of these ionograms is presented in detail as a way of leading to a better understanding of HF radiowave propagation. Special emphasis is placed on a description of the effects of ionospheric clutter and sporadic-E on the performance of the radar.

14. SUBJECT TERMS

High Frequency; Radiowave Propagation; Ionosphere; Backscatter Ionogram; Clutter; Sporadic-E

15. NUMBER OF PAGES
38

16. PRICE CODE

17. SECURITY CLASSIFICATION OF REPORT	18. SECURITY CLASSIFICATION OF THIS PAGE	19. SECURITY CLASSIFICATION OF ABSTRACT	20. LIMITATION OF ABSTRACT
Unclassified	Unclassified	Unclassified	SAR

NSN 7540-01-280-5500

TABLE OF CONTENTS

DTIC QUALITY INSPECTED 3

LIST OF FIGURES

1.0 INTRODUCTION

This report summarizing the High Frequency Radiowave Propagation was prepared, as part of a larger effort by the scientific community to publish a comprehensive "handbook" for use by the U.S. Air Force Over-the-Horizon radar operators at all levels, from technicians on up, that have had only a minimal exposure to the fundamentals of HF radiowave propagation in an ionized medium, the mechanics of the radar and the structure of the ionosphere and its relationship to other geophysical phenomena. The focus of this report is on the application of the fundamentals in these disciplines to the successful operation of the radar, bringing together the several areas of expertise necessary to make a very complex field more understandable.

The need for this material was often illustrated by the "folklore" circulated amongst the operators to explain certain phenomen that did not seem to fit their preconceived understanding of how the radar, the HF radiowave and the ionosphere interacted with each other. At times this resulted in operation of the radar that was less than optimum and it was felt that their overall performance would improve when these operators have access to this type of material.

This work depended on the contribution of several people who took the time and effort to discuss and review this report.

2.0 HIGH FREQUENCY (HF) RADIOWAVE PROPAGATION

2.1 Introduction

High frequency radio waves (3 to 30 MHz) are reflected, or more correctly, refracted by the ionized layers of the upper atmosphere. OTH radar systems, operating in this frequency range, are used to detect long range (500 to 1800 nm) aircraft targets. A small fraction of the total incident energy from the radar is backscattered by the moving target and returned to the radar over the same propagation path taken by the signal traveling out to the target. This same ionosphere, which makes it possible for the over-the-horizon radar to detect long range targets, accounts for a major part of the difficulties encountered in OTH radar operation. The two major problem areas are:

1. Understanding ionospheric phenomenology as it impacts on frequency management of the radar (operating frequency selection).

2. The sources and structure of ionospheric electron density irregularities, generating radar clutter and it's effects on radar performance.

Both of these areas are discussed in detail in this report to provide the OTH radar operator with a reference for comparison with their actual operating experience. This information is necessary so that the operators can be as knowledgeable as possible about the ionospheric propagation situations that will be encountered on a routine basis.

This report puts together a workable model of the characteristics of HF radiowave propagation and how these characteristics are related to the needs of the radar operators (ionospheric assessment and frequency management) at an OTH-B Radar Operations Center. This report covers situations that these operators may expect to encounter using the perspective of people who have used these systems in the past and have, in addition, an understanding of the environment in which these radar operate.

2.2   Basic Propagation Theory

An important part of the understanding of the nature of the interaction of a radio wave with the ionosphere is to understand the structure of the ionosphere itself.

The OTH-B radar frequency manager must select an operating frequency that provides the best possible "coverage" at any particular time. "Best possible coverage" is defined in terms of putting the radar's energy at the required range to achieve, for a specified target size, a signal-to-noise ratio sufficient to ensure a high probability of detecting (establishing a track) any aircraft in the illuminated area at the particular time.

To understand basic theory of radiowave propagation, we start with a simplified ionospheric layer. A parabolic-shaped layer will be used here since it closely resembles actual layers having a maximum electron density at a particular altitude. The ionosphere can be represented quite accurately by several parabolic layers of varying peak densities, altitudes and thickness.

To introduce the basic concepts, a single layer is considered first. To further simplify this analysis, a flat earth model is also used. Three parameters are necessary to define the general parabolic layer: the maximum electron density, expressed in terms of the plasma frequency; the height above the surface of the earth at which the maximum is found; and a measure of the thickness of the layer.

For the parabolic layer (parabolic in electron density), the plasma frequency, f_p, which is related to N_e, the electron density, through a quadratic relation, $f_p \propto N_e^{0.5}$, is as a function of altitude z:

$$f_p = f_o \sqrt{1 - \left[\frac{z - h_o}{Y}\right]^2} \tag{1}$$

where f_o is the maximum plasma frequency (also called the layer critical frequency), h_o is the height of the maximum plasma frequency above the surface of the earth and Y is the semi-thickness, i.e. the height above and below h_o where $f_p = 0$.

The parabolic-shaped layer is shown in Figure 1 and is specifically chosen for this example because there exists an analytic solution, that is a mathematical relationship, that describes the propagation characteristics (ground distance and group path/slant range/radar range; for definitions see below) of any ray launched from the radar and its path through the ionosphere, either penetrating the layer or reflecting and propagating to the ground (target).

The ground range is the measure of the range of a ray, in kilometers or nautical miles along the surface of the earth, from the origin of these rays (for this example the radar) to the point where the ray again reaches the surface of the earth (non-penetrating ray).

The group path, slant range or radar range (all are common names for the same quantity) describe a more complicated concept. It is necessary to understand that the "range " to an aircraft target or to a ground point as determined by the radar is always, in fact, a measure of the time delay for the transmitted pulse (see Scientific Report #7, PL-TR-92-2134) to travel from the radar to the target and back again. Since this path describes a trajectory where the radar pulse travels obliquely up to the ionosphere and then reflects back down to the target, the group path is always longer than the previously defined ground range. However, this difference is just a simple geometrical calculation, if this was the only factor, the conversion from slant range to ground range would be straight forward.

What makes this conversion process more complicated is that converting the measured time delay to a distance requires some assumption as to the speed of the radar pulse along it's path from the radar to the target. It has been tacitly assumed that the character of the path is reciprocal, in that the return path (from the target to the radar) is identical to the out-going portion. This assumption is generally correct. The conversion of the measured time delay to group path or radar range always assumes that the radar signal travels along it's entire path at the velocity of light in a
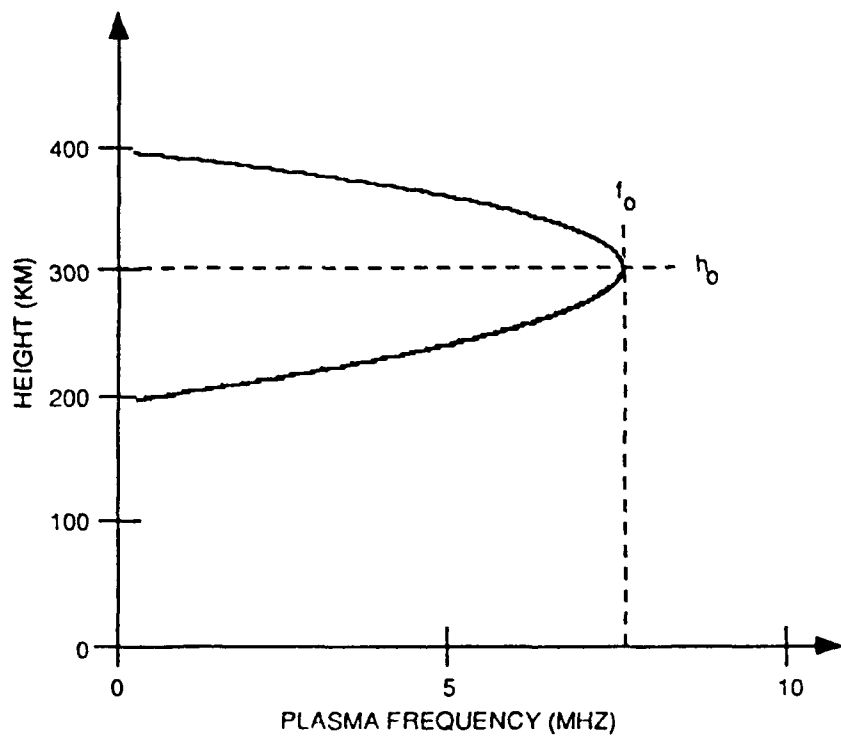
4

Figure 1. Parabolic Layer

5

vacuum, i.e. $c=3 \times 10^5$ km/s. In fact this is not correct as a portion of the path is in the ionospheric plasma where the pulse propagates at velocity less than the "c". The speed of the pulse varies with the ambient electron density and changes as the ray propagates into the ionosphere. It is this consideration which makes the conversion of the radar range to true ground range (this process is called coordinate registration) very difficult. This conversion requires a knowledge of the ionospheric medium along the ray path from the radar to the target. There are several techniques for accomplishing this conversion from radar range/slant range to ground distance, with varying degrees of sophistication and difficulty.

Before discussing the exact solutions for an electromagnetic wave propagating along a path through such a parabolic layer, let us look at a typical ray set (Figure 2) for a frequency greater ($f = 2 \times f_0$) than the critical frequency of the layer. For this particular ray tracing it is assumed that the ionosphere does not change with distance along the path from the radar to the target. In this figure, a minimum takeoff angle θ_{min} is indicated, below which no rays are traced. The transmit and receive antenna patterns describe the "gain" of the antenna array as a function of elevation angle, i.e. $G(\theta)$ (see discussion in Interim Technical Report #6). Actual transmit and receive antenna systems have a minimum elevation angle below which they radiate relatively little power and cannot be used at those angles for target detection. From the ray patterns, it can be seen that the lowest elevation angles provide the longest range coverage. The antennas of the OTH system have been designed to radiate most of the radar's energy at angles that provides the optimum long range illumination. Rays above a certain elevation angle, $\theta_{penetrate}$, penetrate the ionospheric layer; depending on the parameters of the layer and the radar operating frequency. These rays also do not contribute to the radar coverage of aircraft targets.

From Figure 2, the ground range of a ray, that is, the distance from the radar to where the ray returns to the ground, increases as the elevation angle decreases. These low angle rays deliver the longest ranges consistent with sufficient radiated power for effective target detection. Conversely, as the elevation angle increases, the ground range decreases reaching a minimum range, somewhat before the rays
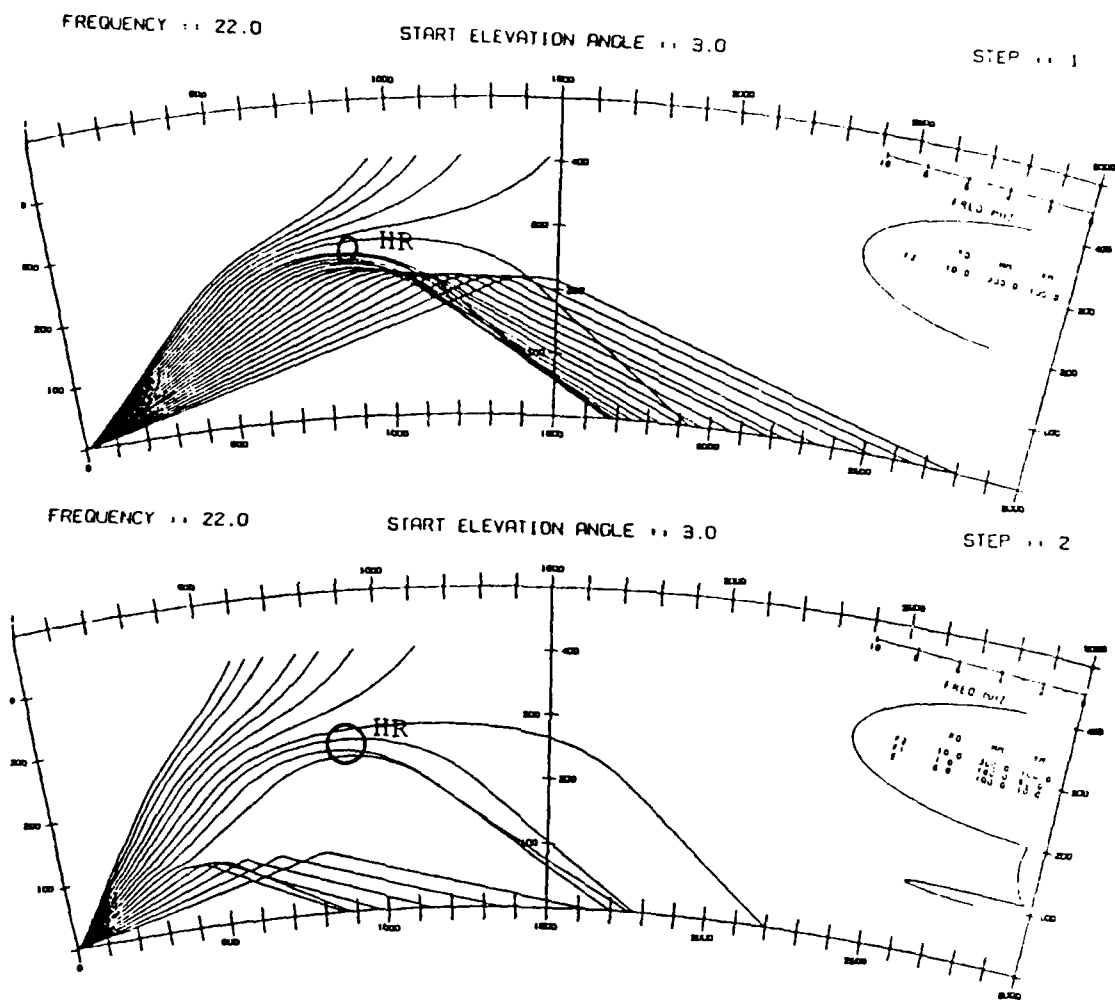
FREQUENCY :: 22.0   START ELEVATION ANGLE :: 3.0   STEP :: 1

FREQUENCY :: 22.0   START ELEVATION ANGLE :: 3.0   STEP :: 2

Figure 2. Basic Ray Tracing
(a) F-Region
(b) E-Region

penetrate. The elevation angle associated with this minimum range is designated as θ_{skip}. The distance from the radar to the minimum ground point is called the skip distance for the obvious reason that no energy from the radar falls into the interval from the radar to the skip distance and all targets in that area are undetectable as long as the radar operates at the particular frequency or until the parameters of the ionosphere change and the skip distance changes.

For elevation angles $\theta > \theta_{penetrate}$ the rays penetrate the ionospheric layer; that is these rays are not refracted (reflected) back towards the ground from the ionospheric layer. For the small range of elevation angles between θ_{skip} and $\theta_{penetrate}$, the radiowaves are refracted back to the earth via paths, which travel close to the peak of the layer. They are called "high" rays and reach the ground at distances greater than the skip range. Only the high rays which land close behind the skip carry any significant energy and are therefore of any relevance to the operation of the OTH radar. For ranges just beyond the skip distance, the high and low rays ($\theta < \theta_{skip}$) can make a target appear as two targets, because the high ray travels a longer time (slant range) than the low ray to the same target.

As mentioned earlier, the term reflection is often used when describing the ray paths from the radar to the target. Technically, reflection should be applied only when the propagation is similar to a light beam incident on a mirror where the ray travels along a straight line path towards and away from the mirror. For ionospheric propagation these conditions are almost met when sporadic E (E_s) is present with little ionization below the layer and the layer has a large electron density gradient with height at the reflection point. The more typical case of ionospheric propagation is within a slowly changing electron density medium which leads to a gradual bending (refraction) of the ray, ultimately turning it around, depending on the incidence angle and the operating frequency relative to the layer critical frequency, back towards the earth. Here, the reflection point is the apogee (highest point) along the ray path.

Target coverage can be maintained from the skip range out to the maximum range determined by the minimum useful elevation angle. In fact, for the actual curved earth case, even for an elevation angle of 0° there is a maximum range which depends only on the height of the reflecting layer. For an F-layer reflection this

maximum range is about 4000 km (h_mF= 300 km) and for an E-layer reflection the maximum range is about 2200 km (h_mE = 100 km). Figure 2a illustrates a typical ray set, for a single F-layer model, and the maximum achievable range. For the flat earth model θ = 0 is meaningless, since the ray can never reach the ionosphere and a lower limit must be set at some θ_{min} (the characteristic of the radar antenna systems discussed above) and which also applies in the curved earth situation.

As stated earlier, the ionosphere, initially, is assumed not to change along the ray path (horizontally stratified); i.e. there are no changes in the electron density profile along the ray direction as one moves away from the radar. For the curved earth, the equivalent condition is that the ionosphere is spherically concentric with the earth. Under these conditions, the elevation angle of the ray as it reaches the ground at the range of the target is the same as when it left the radar site. When a tilted ionosphere or horizontal gradients (the ionosphere is not horizontally stratified) in the layer critical frequency are considered, the assumption of equal angles is not correct.

Figure 2b shows the effects of adding a second lower layer, in this case a 6 MHz sporadic-E layer. Here, the lowest elevation angle rays are "cut off" by the lower layer reducing the span of ground coverage achievable by the normal F-mode. This results in a narrowing of the F-mode radar barrier coverage. This reduced coverage is replaced by short range Es-mode coverage.

Continuing with the flat earth model (this model is reasonably valid only out to relatively short ranges, 1000 km, but it is useful for illustrative purposes), we now look at the exact solution for the ray path through a parabolic layer. There are several versions of this solution (Budden, Kelso, etc.) and here, the one presented by Kelso is used. The equation for the ground range as a function of elevation angle is given as:

$$D = 2\, h_o \left[\frac{f}{f_o}\right] \sin(90-\theta)\, \ln \left[\frac{1 + \left[\frac{f}{f_o}\right]\cos(90-\theta)}{1 - \left[\frac{f}{f_o}\right]\cos(90-\theta)}\right] + 2(h_o-Y)\, \tan(90-\theta) \qquad (2)$$

where f_0 is the maximum plasma frequency of the layer, θ is the ray elevation angle, h_0 is the height of the maximum plasma frequency (electron density) and Y is the semithickness of the layer. The horizontal projection of the straight line portions of the ray path propagating below the ionospheric layer must be added to the path length in the ionosphere to obtain the total ground range for the rays.

Figure 3 is a plot of the calculated ground range as a function of elevation angle θ, obtained using a typical ray set with an operating frequency, for this example, of $f=2 \times f_0$, a maximum layer height $h_0=300$ km and a semithickness $=100$ km. In Equation 2, it is important to recognize that the radar operating frequency always appears as the ratio f/f_0, that is relative to the layer critical frequency, and that, besides the parameters of the ionospheric layers, only the ray elevation angle θ is required to compute the ground distance.

A plot of D as a function of elevation angle θ for a several values of f/fo is shown in Figure 4. Note that the minimum range corresponding to the skip distance changes with respect to the normalized operating frequency, f/fo. Beyond the skip range, the ground range of the rays increases continuously with decreasing θ until θ_{min} is reached.

In Figure 3 and 4 it is apparent that for any range greater than the skip distance, there are actually two solutions to the ray calculation; one for $\theta < \theta_{skip}$ and a second solution with $\theta > \theta_{skip}$, but of course less than the angle for which all rays penetrate the layer. This means that, at any frequency, to any ground range beyond the skip distance, there are two different rays with different take-off angles that reach that particular range. These two solutions are designated as a high ray ($\theta_{penetrate} > \theta > \theta_{skip}$) and a low ray ($\theta < \theta_{skip}$). For most purposes it is the low rays that are involved in radar detection, while the high rays, which are considerably weaker, are considered a nuisance whenever they are present.
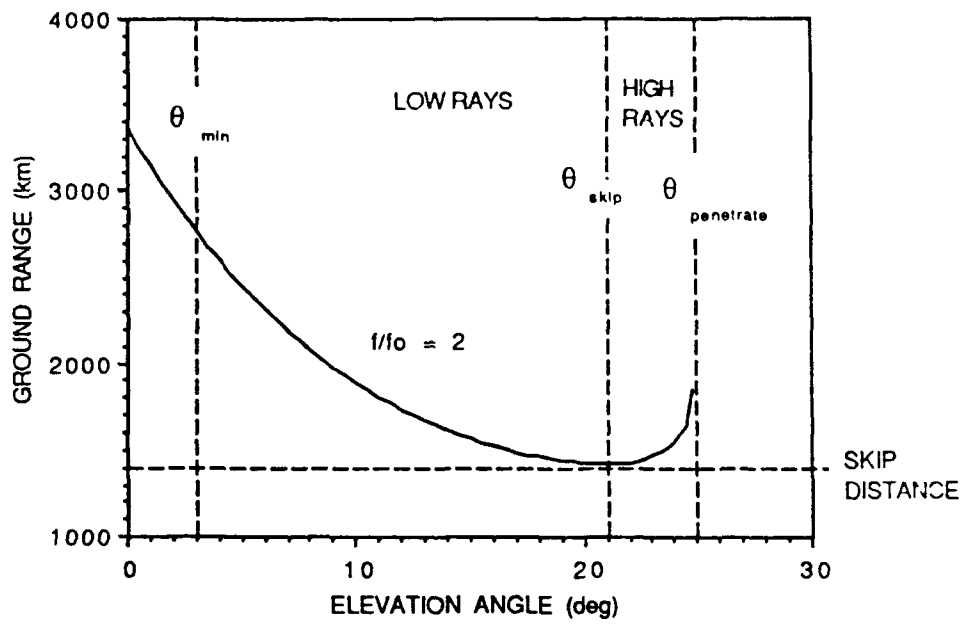
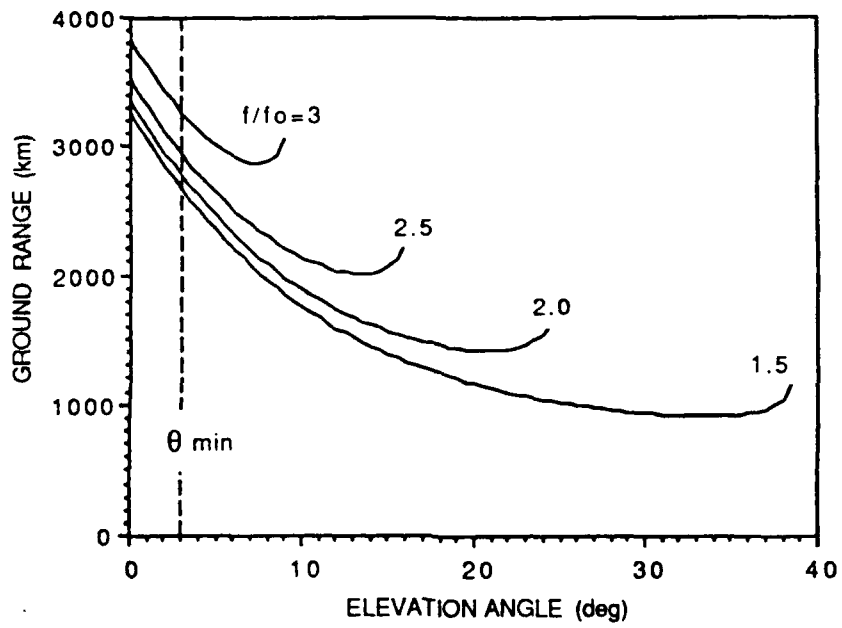Figure 3. Ground Range vs. Elevation Angle-Single Parabolic Layer

11

Figure 4. Ground Range vs. Elevation Angle-Function of Operating Frequency

High rays are so named because their reflection height and take-off angle are always greater than those for the other (low ray) solution. A few high rays are indicated in Figure 2. The fact that the high rays are inherently weaker can be seen by examining their ray density in Figure 2. Here all the high rays originate in the relatively small elevation angle interval designated HR in the figure. The energy contained in the total bundle of high rays is proportional to the angle interval, $\theta_{penetrate} - \theta_{skip}$. For the same range interval, for example, from the skip distance out to 3,000 km, the low rays cover a much larger elevation angle interval from $\theta_{skip} - \theta_{min}$ indicating a higher signal amplitude. Only near the skip distance does the high ray intensity approach the low ray intensity. At the skip range the two modes merge and the signal is the sum of the two equal signals.

Using Figure 4, for several operating frequencies ($f = 1.5 \times f_o$, $2.0 \times f_o$, $2.5 \times f_o$ and $3.0 \times f_o$), a plot of the skip distance as a function of frequency (Figure 5) is presented. Two important characteristics of HF propagation become immediately obvious:

1. The skip distance increases as the operating frequency is increased for fixed ionospheric parameters. Using this fact, it is possible to provide OTH-B radar coverage for any desired range interval by selecting the proper operating frequency at any particular time. For example, if the desired range start is 2,200 km, with this particular ionospheric model, the operating frequency should be set at $2.3 \times f_o$. This provides coverage from 2,200 km out to the maximum range consistent with the minimum available antenna elevation angle.

2. The elevation angle associated with the skip distance decreases as the operating frequency increases. Implied in all the previous discussion is the assumption that the antenna gain in the vertical plane is relatively constant over a wide range of elevation angles down to θ_{min}. This ensures a relatively uniform illumination for targets at all ranges within the coverage region.
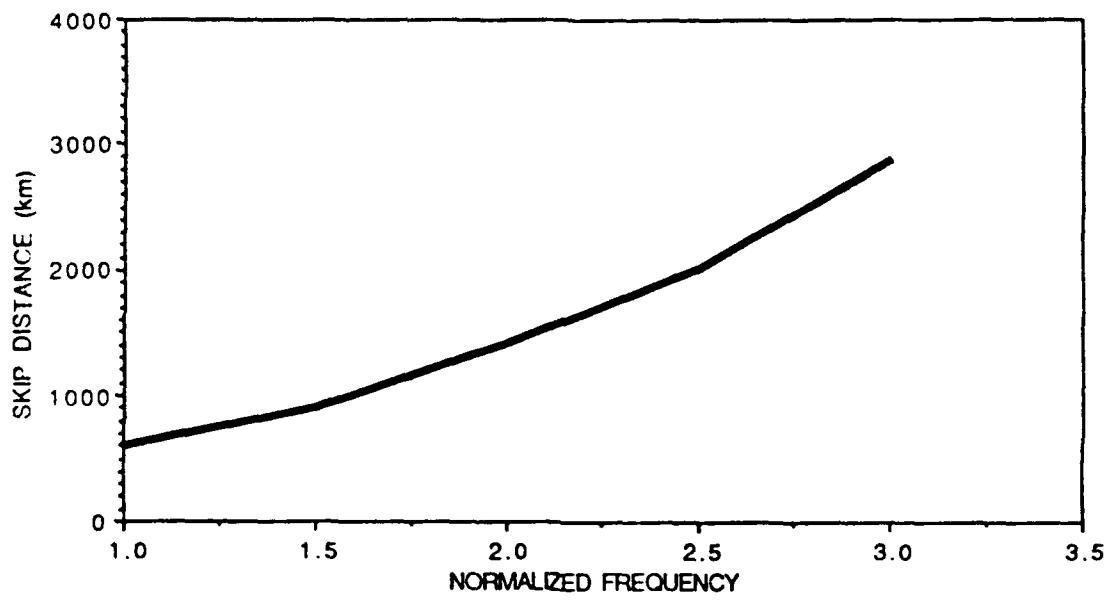
13

Figure 5. Skip Distance vs. Operating Frequency

14

To illustrate how these calculations can be combined in this simple case to generate a backscatter ionogram, three sample ray tracings are displayed in Figure 6(a) for three different frequencies. In Figure 6(b) the ground coverages derived from the ray tracings are converted to the slant range vs. frequency plot. These data are shown as vertical line segments for the ground ranges achieved at each frequency. If it is assumed that this ray tracing process is repeated for all sounding frequencies, then the one hop ground coverage area on the backscatter ionogram is generated and is indicated here as the shaded area.

The ray tracings can be extended to the two hop situation and by the same process it is possible to develop the two hop ground coverage on the backscatter ionogram. Included in this simplified construction is the vertical ionogram made at the radar site. In practice, if the sounder begins it's frequency sweep at a sufficiently low frequency, some of the radiated energy "leaks" into the vertical direction and a quasi-vertical ionogram (considering the 100nm separation between transmitter and receiver) is produced at the low frequency end of the backscatter ionogram. It is important to observe that the one hop ground backscatter trace begins with the same time delay as the second hop vertical trace. Later, when ionospheric clutter is discussed, it is shown that the ionospheric clutter trace begins at the one hop vertical trace. Similarly, the two hop ground scatter begins out of the four hop vertical trace. This information can be used as a guide to identifying the types of traces seen on the backscatter ionograms.

All the elevation angle-time delay calculations were made using the flat earth model and although these results are only approximately correct, they are instructive and give a qualitative description of HF wave propagation for a typical ionospheric layer.

2.3   Slant Range

As part of the discussion of the slant range to a target using a curved earth model, it is useful to review the concept of slant range. In order to correlate the observed radar track for a particular target with the known flight plan/path of an aircraft, it is necessary to convert the observed slant range to the corresponding ground range.
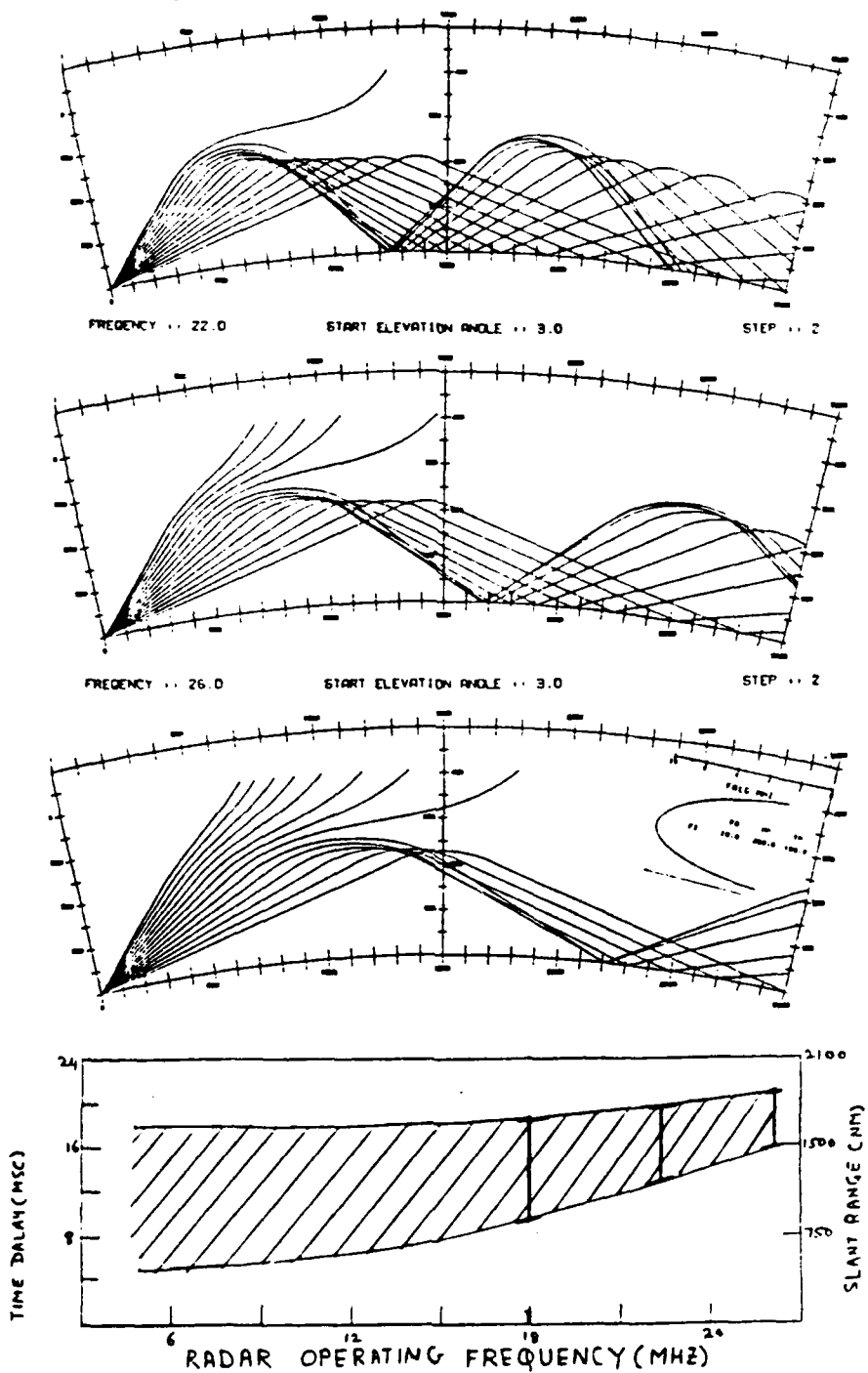
15

FREQ = 18

FREGENCY ·· 22.0   START ELEVATION ANGLE ·· 3.0   STEP ·· 2

FREGENCY ·· 26.0   START ELEVATION ANGLE ·· 3.0   STEP ·· 2

Figure 6. Backscatter Ionogram Construction

16

As discussed earlier, this inversion process requires a knowledge of the structure of the ionosphere, information which is often very difficult to acquire and involves ionospheric profile modeling. At this point it is only necessary to remember that all of the height and range coordinates on ionograms, vertical or backscatter, involve slant ranges and are not the true ground distances or vertical heights.

The difference between slant range and ground range varies from 50 to 200 km depending on the ionospheric profile, range to the target and the radar's operating frequency. Using a simple parabolic model, it is possible to compute the slant range (time delay) to a fixed ground point as a function of frequency and thereby establish a relationship between the slant range and the ground distance.

Figure 7 illustrates Breit and Tuve's theorem, again using the flat earth scenario. The actual ray path is a composite of two straight line segments, OA and CD, and a curved trajectory ABC, along which the radar pulse travels at the group velocity in the ionosphere, slower than the speed of light in a vacuum c. Breit and Tuve state that the slant range, $P' = D \csc\theta_i$, where θ_i is the angle a virtual ray (a straight line ray with the same take-off angle) makes with the local vertical at the virtual reflection height (where the straight ray reaches the midpath point), which means that the time it would take to travel the path OAGCD in free space at the speed of light is the same as the time it takes the signal to propagate along the actual path OABCD through the ionosphere. For the simple case of a flat earth $\theta_i = 90-\theta_o$, where θ_o is the elevation at the ground. For the curved earth case this is not true, but a simple geometric relationship connects the two angles. The height MG is the virtual reflection height which is always greater than the the actual reflection height and can at times be greater than the maximum height of the peak of the layer.

2.4 Backscatter Ionogram Synthesis

The backscatter ionogram provides the primary tool to understand the existing propagation situation under which the radar has to operate. A thorough discussion of the structure of the backscatter ionogram is therefore appropriate for this purpose and to provide a background for the interpretation of the backscatter ionograms used by the EA operators for frequency management.
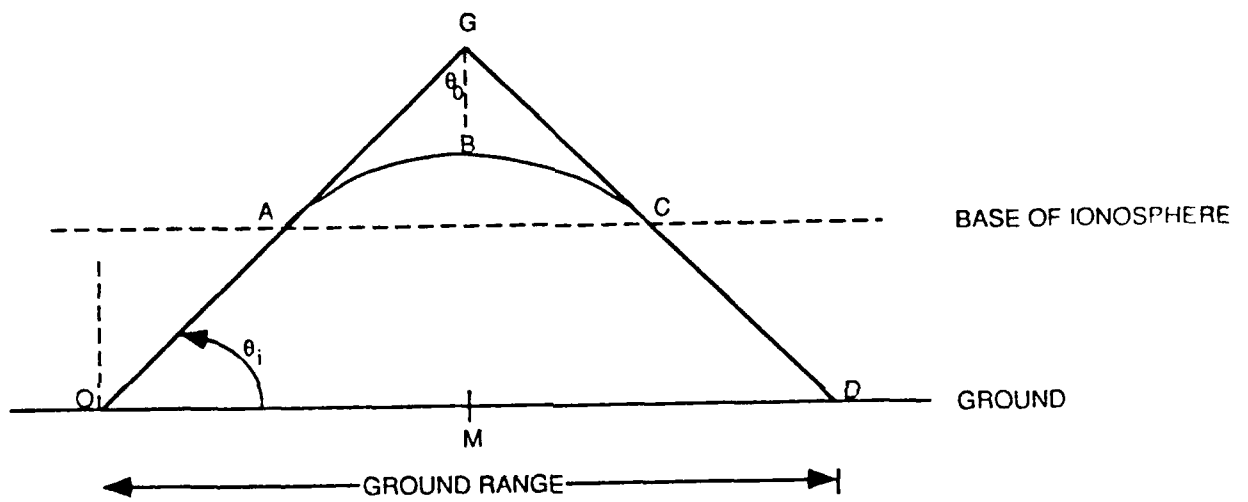
Figure 7. Breit and Tuve Theorem

The backscatter sounder is an instrument designed to indicate, as a function of frequency, the range extent of the ground illumination. The backscatter sounder is a low power swept frequency radar (P_TG_T=50 dBW; see Scientific Report #7, PL-TR-92-2134, for a discussion of the effective radiated power) compared to the actual operational radar. However, this power level is sufficient, since the sounder is designed to detect only the very large cross-section of the illuminated ground area. The conceptual generation of a backscatter ionogram has been discussed in Section 2.2 and Figure 6.

Figure 8 is an example of a backscatter ionogram from the ECRS displaying the slant range to the ground as a function of frequency. The sounder sweeps over a range of frequencies within the 2 to 30 MHz interval, covering the operating frequency range of the radar. The normal backscatter ionogram shows ground backscatter returns out to a slant range of 2000 nm (3750 km). The dark areas indicate strong backscatter return. For each frequency there is a range interval of no backscattered signal corresponding to the skip region for that frequency. When the time delay corresponding to the skip distance is reached, the ground clutter amplitude increases rapidly (see Figure 8) and then decreases relatively slowly as the range increases until for the lowest elevation angles (longest ranges) the decreased antenna gain and geometrical spreading of the sounder energy causes the backscattered signal to decrease relatively rapidly.

Again it is important to remember that the ordinate scale is in terms of group delay/slant range and not ground distance. This difference is less critical for the analysis of the backscatter ionogram than for the coordinate registration process. For backscatter ionograms, approximate corrections from slant range to ground range can be made by simple subtraction of a typical value, which for F-region propagation and typical barrier distances, is 100 nm (185 km). For example when it is decided that the radar operating range (ground distance) should begin at 1100 nm, then the required slant range on the ionogram should be read at 1200 nm.

A catalogue of simulated backscatter ionograms has been computed for the ECRS situation, in 30° azimuthal increments, for summer, equinox and winter, in 4 hour steps and for low (Rz=25), medium (Rz=75) and high (Rz=150) sunspot numbers.
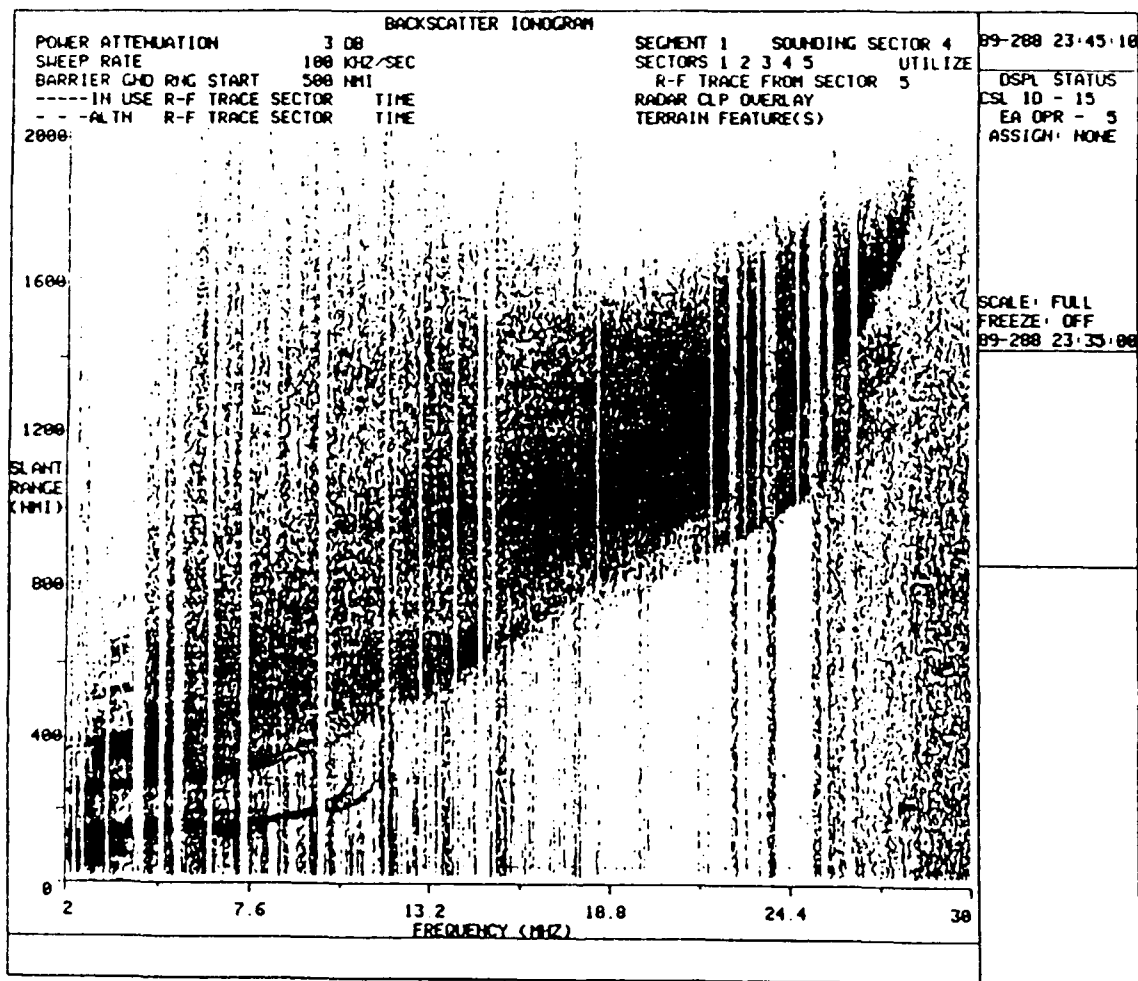
Figure 8. Sample Backscatter Ionogram

This catalogue provides a tool for the operators to understand the typical diurnal variations as well as indicating the azimuth, and solar cycle dependences.

The synthesis of the complete backscatter ionogram is relatively straightforward using ray tracing methods and the derived data presented in Figure 4. For fixed ionospheric conditions, that is, time of day, season, sunspot number, location and direction, the only variables are frequency and ground range. In order to simulate a backscatter ionogram, it is assumed that the surface of the ground is made up of small targets, spaced in range, each capable of scattering back a small fraction of the sounder energy incident on them. For a real ionogram there is, in general, a continuum of ground and sea irregularities which contribute to the backscattered energy received by the sounder. A smooth surface, land or sea, produces little or no backscattered energy. For the case of the sea surface, it is the surface wave structure that provides the irregularities responsible for the backscattered energy.

Two factors outside of the control of the sounder affect the magnitude of the received backscattered power. One is the roughness of the scattering surface and the second is the conductivity of the surface medium. Low ground conductivity produces a weaker returned signal level. The highest conductivity is sea water followed by land where the conductivity is highly variable, depending on water content of the soil. A good example of very a low conductivity surface is the Greenland icecap. Here the backscattered energy can be so small as to make Greenland appear as a "hole" in the surrounding sea.

Before discussing the actual simulation, it is necessary to consider the modeling of the ionosphere for the curved earth case. Here, to generate realistic results, changes in the ionospheric profiles along the "look" direction of the sounder are considered. An ionospheric median synoptic model called IONCAP developed by The Institute of Telecommunications Sciences in Boulder, Colorado is used. This code uses a realistic monthly median global description of the ionosphere along with a rapid ray tracing capability. All synoptic models are not able to describe any of the details of the local spatial or temporal structure within the ionosphere. Only a network of real-time sounders in the coverage area of the radar can achieve this kind of description. For the purposes of understanding the generation of backscatter ionograms and their variations in space and time, the IONCAP model is quite

21

adequate. Although the ionosphere is allowed to vary along the ray path, it is assumed for the purposes of processing speed that for any individual ray, the ionosphere is locally horizontally stratified and can be represented by the midpoint model values.

The received power is calculated from the basic radar equation. The received power is:

$$P_R = \frac{P_T\, G_T\, G_R\, \lambda^2\, \sigma_G}{(4\pi)^3\, R^4\, L^2} \quad [W]$$

(3)

where:

P_T=the transmitter power [Watts],

G_T=the maximum transmitting antenna gain,

G_R=the maximum receiving antenna gain,

λ=the free space wavelength [m],

R=the slant range to the ground point [m],

L=the one-way loss including absorption and other attenuation factors
included in the IONCAP program,

and finally, as the only difference from the earlier discussion of the radar equation:

σ_G=the effective ground area [m^2] contributing to the measured backscatter energy.

The actual ground area contributing to a single slant range (time delay) measurement is a function of the receive antenna beamwidth and the transmitted pulse width. The effective ground area is expressed as a product of a backscatter efficiency and the actual ground area.

A simplified expression for this area is:

$$R\Phi_B \bullet \frac{c\tau}{2} \cosec\,\theta$$

(4)

22

where R is the range as defined earlier, Φ_B is the 3 dB azimuthal beamwidth, θ is the elevation angle and τ is the pulse width. Using typical values for the pulse width of 100 μs, a beamwidth of 2.5 degrees and a range of 2,500 km the illuminated area is 5.1×10^9 [m^2]. The backscattered cross-section, σ_G, used in the radar equation, takes into account the backscatter reflectivity of the surface. This efficiency (backscatter reflectivity) depends on the surface conductivity and roughness; for sea water the reflectivity is typically 5×10^{-3}. This represents the fraction of the total energy falling on this area that is available for backscatter. This value is an upper limit and can become smaller when the wave structure on the surface becomes smaller. For land or ice the reflectivity can vary from 10^{-3} to 10^{-5}. Therefore, for sea water, which is the typical situation for the OTH-B radar system, the resultant backscatter cross-section area is 2.6×10^7 [m^2]. The radar/sounder simulation program computes this effective area for each range and uses it in the radar equation to determine the received power.

The final output of the program is signal-to-noise ratio, where the noise level is determined from standard tables included in the program. These tables, for atmospheric and man-made noise, a function of time, season, location and frequency, were developed by the international radio community and have some limitations which affect their applicability in evaluating radar performance. This noise data base is limited in that, first, the measurements were not made uniformly over the globe, often leaving large areas that had to be filled in using extrapolation techniques and theoretical models. A second important factor that affects the applicability of this data base to the OTH-B radar system is that the standard noise measurements in this data base were made using omni-directional receiving antennas, while the OTH radar system uses highly directive antenna beams. This means that the measurements for the noise data base typically over-estimate the total received noise power.

A simple case is used first to illustrate the construction of the backscatter ionogram. It is important to see this construction detail since it describes structure within the backscatter ionogram which is almost always hidden in the real ionogram. Only through the study of these simulation processes can a useful understanding of these ionograms and of the OTH propagation scenario be attained.

23

As a point of reference, another actual backscatter ionogram is presented in Figure 9. These data were taken from the USAF ECRS on Day 299, 1990 at 2031 UT. The particular example shown was obtained in late fall in the afternoon.

As discussed earlier, these backscatter ionograms are used to select the approximate operating frequency after a range start for the radar coverage is established. A horizontal line is drawn across the ionogram at the desired range start, after the appropriate correction for the slant range/ground range conversion. The intersection of this horizontal line with the leading edge determines the maximum frequency that can be used to illuminate the ground at the desired range and beyond, at that particular time and azimuth.

For the particular example in Figure 9, the maximum frequency would be 24.5 MHz for a range start of 800 nm. The leading edge represents the minimum time delay (skip distance) as a function of frequency. The general behavior of the leading edge with frequency is the same as illustrated in Figure 5. The darkened area at longer time delays than the skip represents potential coverage by the radar and is primarily low ray illumination.

A qualitative estimate can be made, using these ionograms, as to the available barrier width, that is, how far beyond the range start is detection performance likely to be acceptable. In this case, at 24.5 MHz, time delays out to 1200 nm have some degree of darkening and likely represent sufficient signal-to-noise for good aircraft detection. This yields a barrier width of about 400 nm. Some frequencies would have wider barriers and others more narrow barriers. This is only a qualitative estimate as the radar's sensitivity is much greater than that of the backscatter sounder and this cannot easily be translated to the backscatter ionograms.

For the simulation of backscatter ionograms, the approach taken here was to use a set of equally spaced frequencies and carry out a set of ray tracings using equally spaced elevation angles with ionospheric profiles derived from the IONCAP synoptic model. For each frequency, the density of these rays as they reach the ground is used as a measure of the strength of the backscattered signal. As previously discussed, the IONCAP ionospheric model uses the electron density
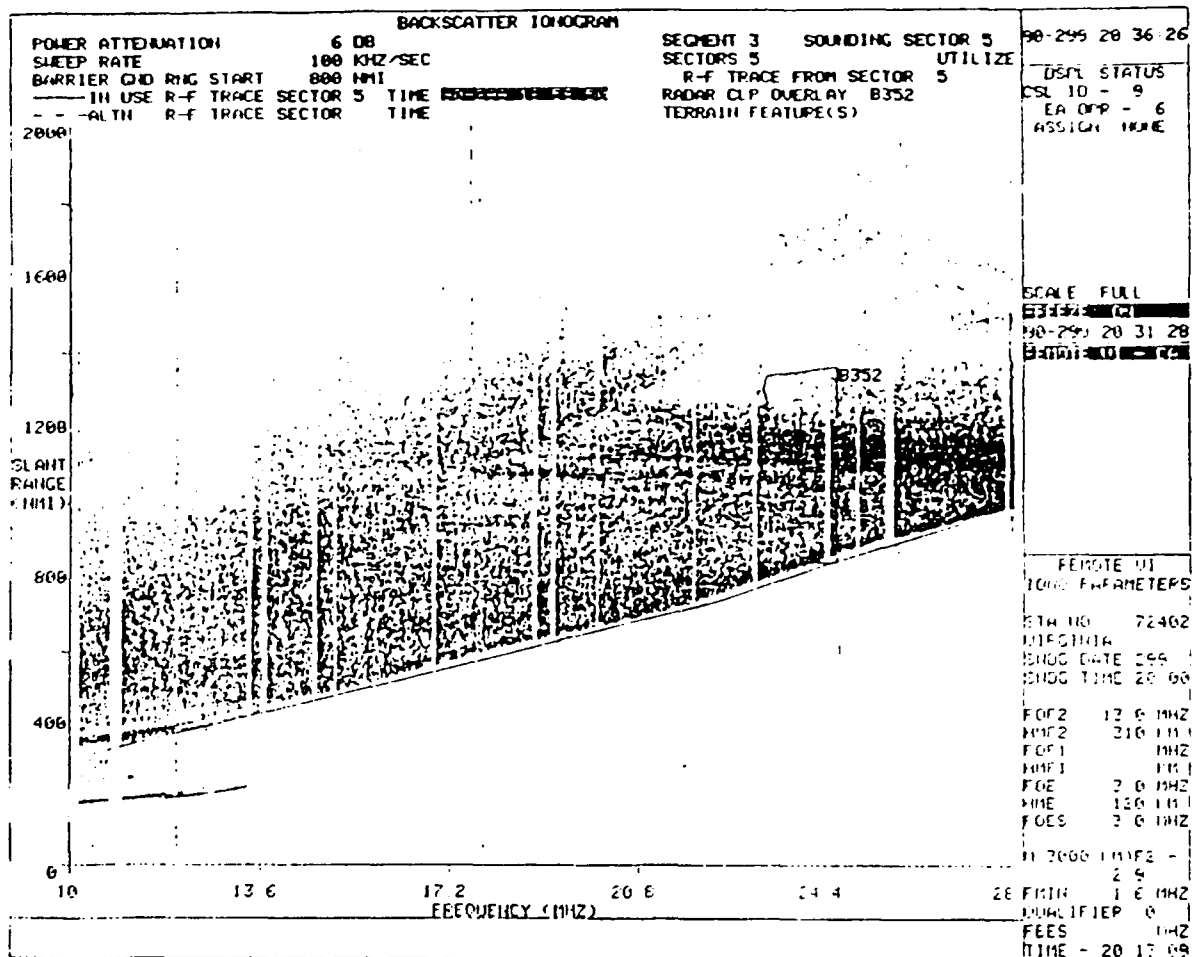
24

Figure 9. ECRS Backscatter Ionogram - (90-299)

profile relevant to the midpoint of each path to the selected set of ground ranges. This is important, as a more realistic ionogram could be computed when the approximate electron density gradients in the model are considered.

The sunspot number (SSN) used in the model corresponds to the level of solar activity in the particular phase of the 10.5 year solar cycle for the period being modeled; this is in addition to the month or season, the time of day, location and azimuth as the other required inputs to the model. Also, the backscatter sounder parameters must be selected for this simulation to model the particular sounding system in use at the radar site. These parameters include P_T, G_T and G_R, as functions of elevation angle, azimuthal beamwidth, pulse width, chirp rate and frequency range. For all the calculations included here, the following parameters were selected:

$P_T = 10$ kW

G_T and G_R using the ECRS sounder antenna gain models

Receive antenna-azimuthal beamwidth = 7.5 degrees

Chirp rate = 100 kHz/s

Frequency range = 2 to 30 MHz. Although the radar sounder start frequency is 5 MHz, it is often instructive to see detail down to a lower frequency such as 2 MHz.

As part of the ray tracing program, the height of the reflection of each ray is identified and the specific reflection layer is assigned to each ray. When the simulated ionograms are printed a different symbol is attached to each point on the ionogram describing the appropriate propagation mode (i.e., reflection by the E, F1, or F2 layer). Figure 10 shows a simulated backscatter ionogram for the ECRS location, the equinoxial season, SSN=75, 16 UT (near local noon) and an azimuth of 76.5° T. The contribution of the three ionospheric layers is apparent in the structure of the backscatter ionogram and illustrate the time delays associated with each of these modes. The configuration of these layers change as the parameters of the model are changed.

Two particular ranges are highlighted in Figure 10 to illustrate the changing mode structure as the ground range increases. The ranges of 1500 and 2500 km were selected and show that the dominant mode controlling the leading edge is the one
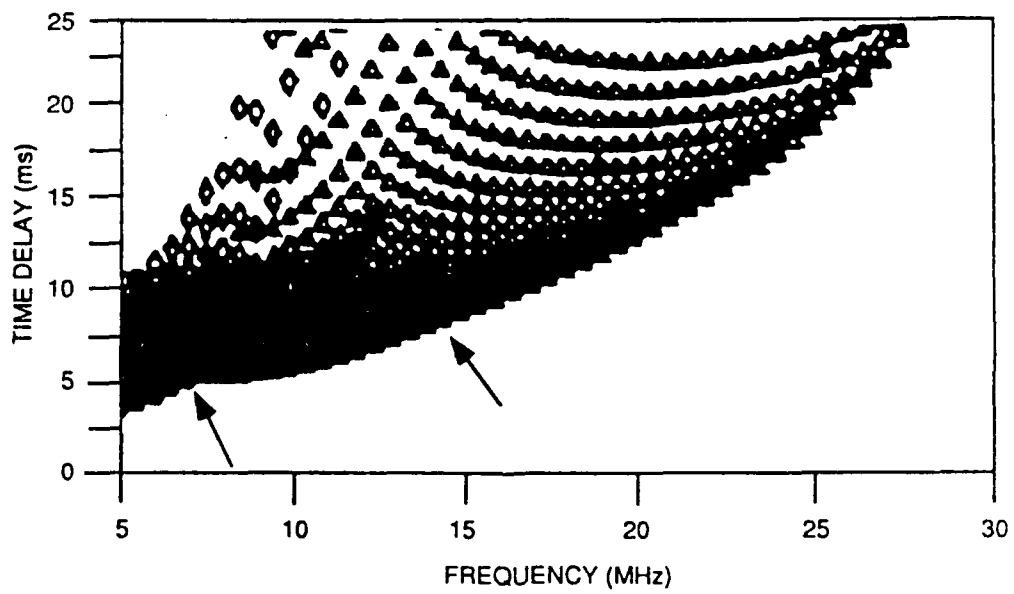
Figure 10. Simulated Backscatter Ionogram

hop E-layer at the shorter range, while at the longer range the controlling mode is the F2 layer. If a composite ionogram, without the layer indications is examined, it is impossible to recognize the different contributions. At other times and in other directions, the mode structure may be more apparent.

It is also essential to remember that these simulations are based on median ionospheric models and considerable variance from the actual ionograms should expected.

2.5   Ionospheric Clutter Effects

In order to complete the picture of the structure of the backscatter ionogram it is necessary to understand backscatter from ionospheric irregularities which can significantly affect the performance of the radar. These unwanted signals, known collectively as ionospheric clutter, result from both the sounder and radar signals being scattered from small scale, quasi-random fluctuations in the ambient electron density. This scattered energy shows up on the backscatter ionogram and produces traces that can often be confused with ground scatter and often masks the actual ground scatter leading edge. The performance of the radar is affected by this spread Doppler clutter obscuring the target signals. This occurs because of the random velocities associated with these irregularities and the backscattered energy appears as Doppler spread clutter which, when added to the radar's ambient noise level, makes it more difficult to detect aircraft targets.

The magnitude of the scattered power depends, intrinsically, on the "shape" of these irregularities, their mean size relative to the wavelength of the radar signal, the intensity of the fluctuations, (i.e. the RMS change in the local electron density relative to the ambient electron density, $\Delta N/N$ (typically $\Delta N/N$ varies from less than 1% up to about 10% for very intense irregularities that might occur in the auroral regions)) and finally on the orientation of these elongated irregularities relative to the radiowave direction at the scattering point, all summarized as the intrinsic backscatter cross-section of these ionospheric irregularities.

28

The total scattered power is determined by the intrinsic backscatter cross-section discussed above as well as by the volume of irregularities that contribute to a particular range cell on the ionogram or radar at the particular operating frequency. The volume that contributes to the clutter power is a three dimensional region determined by the sounder and radar parameters and by the characteristics of the height and range distribution of ionospheric irregularities. The two radar parameters that affect the scattering volume, shown pictorially in Figure 11, are the transmitted pulse width (after compression; see Scientific Report #7, PL-TR-92-2134) and the azimuthal receive beamwidth. To the first order the volume can be written as:

$$\text{SCATTERING VOLUME} = R^* \Phi_B * \frac{c\tau}{2} * \Delta h \tag{5}$$

where R = range to the scattering volume, ϕ_B is the azimuthal beamwidth, c = speed of light, τ = pulse width and Δh is the height extent of the irregularities for a fixed time delay (corresponding to the particular range cell). With typical numbers for these parameters:

$$R = 2000 \text{ km}$$
$$\phi_R = 2.5 \text{ degrees}$$
$$\tau = 100 \text{ } \mu s$$
$$\Delta h = 10 \text{ km}$$

the scattering volume is 1.3×10^{13} m^3. The backscatter cross-section area (m^2) can then be written as the product of this volume (m^3) and the intrinsic backscatter cross-section (m^2/m^3) for the ionospheric irregularities (which depends on the the structure of the irregularities as discussed above).

The calculation of the intrinsic backscatter reflectivity is beyond the scope of this text but the results, which depend on the above irregularity parameters, varies from approximately 10^{-7} to 10^{-13} (m^2/m^3) giving for a final backscatter cross-section for distributed ionospheric irregularities, 1.3×10^6 (m^2) to 1.3×10^0 (m^2). For the larger cross-section values, the ionospheric clutter is comparable with the ground area and given a degree of Doppler frequency spreading, can seriously affect the performance
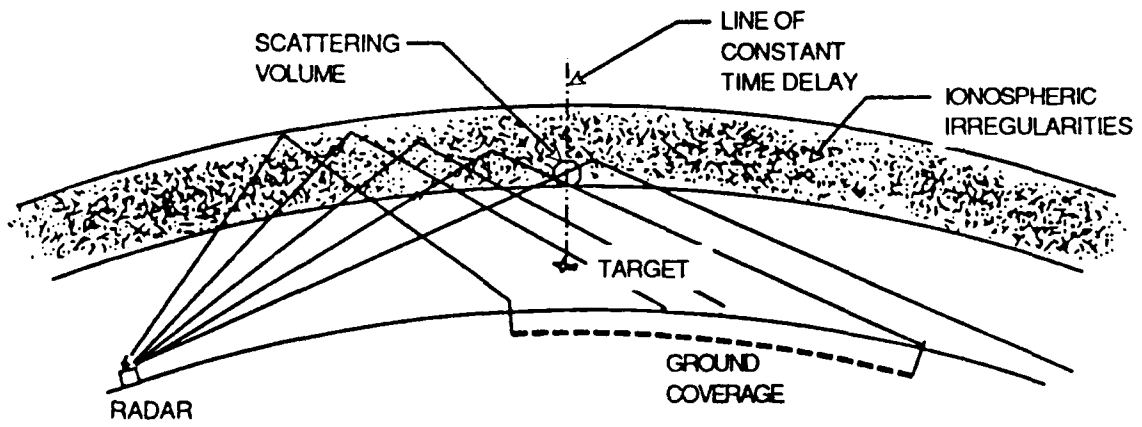
Figure 11. Scattering Volume

of the radar. For the less intense irregularities the backscatter cross-section is six orders of magnitude smaller and is comparable to the background noise level and the effect on radar performance is minimal.

Using the same ionospheric models used to produce the ground clutter plots, it is possible to locate the regions of ionospheric clutter by finding the locations where the same rays used in determining the ground clutter become orthogonal to the earth's magnetic field. The most accepted theory for the origin of the backscatter ionospheric clutter is that strong scattering occurs when the ray is perpendicular to the long axis of the ionospheric irregularities. The dynamics of the formation and growth of these irregularities indicates that there is a strong tendency for these irregularities to become elongated along the local direction of the earth's magnetic field (field aligned), particularly at the higher altitudes in the F-region of the ionosphere. These irregularities can be pictured as ellipsoidal in shape with their long axis aligned with the direction of the local geomagnetic field, which varies with latitude from near vertical at the high latitude regions in the auroral zone to near horizontal at the magnetic equator.

Other mechanisms exist for the formation of ionospheric irregularities such as from the ionized trails left behind by very small meteors entering the earth's atmosphere and burning up in the 100 km altitude regime. These ionized trails also act as elongated scattering bodies with random orientations. These scattering centers are in the E-region of the ionosphere and intercept the rays on their down leg towards the target. It is very likely that other mechanisms for the sources of ionospheric clutter exist and they all must be considered to complete the picture of the clutter problem.

For the case of field aligned irregularities, the method used to determine the location of the ionospheric clutter is to use ray tracing and to find those points where the rays are perpendicular (or nearly perpendicular) to the geomagnetic field along its path. In the more northerly sounding/radar directions this orthogonality occurs when the ray is close to its apogee (near to the reflection point). Each ray contributes to the clutter power, and although the fraction of the total incident energy backscattered out of the beam is small, it is often sufficient to affect the detection of aircraft targets. This happens, not by significantly reducing the energy

31

falling on the targets, but by increasing the background noise level. Although orthogonality is a necessary condition for strong ionospheric clutter, it is by itself not sufficient since the scattering requires perturbations in the local electron density (irregularities) somewhere along the ray path.

Because the backscatter sounder is relatively insensitive, only the strongest clutter sources (large $\Delta N/N$ or favorable scattering conditions) can be seen on the backscatter ionograms, much stronger than the levels that affect the radar's performance. For the radar, the sources of clutter do not have to lie within the unambiguous range interval (see Scientific Report #7, PL-TR-92-2134); usually defined by the one hop region. The sources of clutter often do lie within this primary range interval, for example for the ECRS in Segment I, at night the auroral irregularities are found within the radar coverage. On the other hand, in Segments II and III, the irregularit⁻ ⌐ ⌐sociated with the nighttime activity, in and around the equatorial region, aff⌐⌐ the radar's performance. Here the clutter often lies in the three hop region c⌐ at even longer ranges (10,000 km) from the radar and affects the radar's performance after being range folded into the processed range interval (normally from 1000 nm to around 1500 nm.

2.6   Sporadic-E Effects

One ionospheric layer not considered so far in the discussion of OTH propagation and the generation of backscatter ionograms is the sporadic E layer. As discussed earlier, the sporadic-E layer is a relatively thin ionospheric layer, some 2 to 10 km thick that often appears at unpredictable times, though more often in summer than the other seasons and more often during the daytime, in the altitude regime near 100 km. Sporadic-E is often patchy with an average horizontal structure size of the order of 500 km. This is a large enough area to support radar coverage, however, at a shorter ground range than is usual when the radar is operated in an F-layer mode (see Figure 2). Sporadic-E is characterized by a very large vertical gradient in electron density, i.e. a significant change in electron density over a relatively short height interval (1 to 5 km corresponding to the half thickness of the layer) and is a reflecting layer that often produces good target de.ections, though at the shorter ranges of 500 to 1000 nm as a result of the "low" height of the layer. The significance of the Es to the radar operation results from the fact that while it often provides

32

excellent coverage out to a maximum range of 2000 km (≈ 1000 nm) it prevents the OTH radar signal from reaching the F-layer and providing long range coverage, i.e., from 1100 to 1800 nm.

Irregularities associated with this layer and the normal E-layer produce special effects on the backscatter ionogram that are best described using the same simulation techniques as for the F-region clutter. Again, the E-region irregularities are assumed to be field-aligned and the associated ionospheric clutter location is determined by searching for the points on the ray path that are orthogonal with the geomagnetic field.

Because of the spatially localized nature of Es and with little underlying ionization, an almost constant slant range trace, independent of the sounding frequency, is found on the backscatter ionograms from the ground via the Es layer.